JGR Atmospheres

RESEARCH ARTICLE
10.1029/2018JD030092

Radiative Convective Equilibrium and Organized Convection: An Observational Perspective

C. Jakob[1,2], **M. S. Singh**[2], **and L. Jungandreas**[3]

[1]ARC Centre of Excellence for Climate Extremes, Monash University, Melbourne, Victoria, Australia, [2]School of Earth, Atmosphere and Environment, Monash University, Melbourne, Victoria, Australia, [3]Max Planck Institute for Meteorology, Hamburg, Germany

Key Points:
- The scales of tropical radiative convective equilibrium (RCE) are assessed from observations for the first time
- The tropics as a whole are near RCE on a daily basis
- Organized deep convection is a rare state for regions in RCE and is absent when small regions are in RCE

Correspondence to:
C. Jakob,
christian.jakob@monash.edu

Citation:
Jakob, C., Singh, M. S., & Jungandreas, L. (2019). Radiative convective equilibrium and organized convection: An observational perspective. *Journal of Geophysical Research: Atmospheres*, *124*, 5418–5430. https://doi.org/10.1029/2018JD030092

Received 2 DEC 2018
Accepted 27 APR 2019
Accepted article online 1 MAY 2019
Published online 29 MAY 2019

Author Contributions
Conceptualization: C. Jakob, L. Jungandreas
Methodology: C. Jakob, M. S. Singh, L. Jungandreas
Software: C. Jakob, L. Jungandreas
Writing - Original Draft: C. Jakob
Formal Analysis: C. Jakob, L. Jungandreas
Investigation: C. Jakob, L. Jungandreas
Project Administration: C. Jakob
Supervision: C. Jakob, M. S. Singh
Visualization: C. Jakob, L. Jungandreas
Writing - review & editing: M. S. Singh, L. Jungandreas

Abstract Radiative convective equilibrium (RCE) describes a balance between the cooling of the atmosphere by radiation and the heating through latent heat release and surface heat fluxes. While RCE is known to provide an energetic constraint on the atmosphere at the global scale, little is known about the proximity of the atmosphere to RCE at smaller spatial and temporal scales, despite the common use of RCE in idealized modeling studies. Here we provide the first observational evaluation of the scales at which the atmosphere is near RCE. We further use observations of cloud characteristics to investigate the role played by organized convection in the RCE state. While the tropical atmosphere as a whole is near RCE on daily time scales and longer, this is not the case for any given location. Rather, areas in excess of $5{,}000 \times 5{,}000$ km^2 must be considered to ensure the atmosphere remains near RCE at least 80% of the time, even for monthly averaged conditions. We confirm that RCE is established through the interplay of regions of active deep convection with high precipitation and weak radiative cooling and regions of subsiding motions leading to shallow cloud states that allow strong radiative cooling with no precipitation. The asymmetry in the maximum amount of radiative cooling and latent heating leads to the well-known ratio of small areas of precipitation and large regions of subsidence observed in the tropics. Finally, we show that organized deep convection does not occur when regions smaller than $1{,}000 \times 1{,}000$ km^2 are near RCE.

1. Introduction

On global scales, the time-averaged radiative cooling of the atmosphere by radiation must be balanced by latent heating from condensation and the supply of sensible heat from the surface. This very simple energetic constraint on the global atmosphere has become known as radiative convective equilibrium (RCE). Assuming that much of the latent heating is produced by convective overturning, this simple paradigm can, to first order, explain the vertical temperature structure of the tropical atmosphere (Manabe & Strickler, 1964). It also provides a constraint on the tropical-mean precipitation through the tight coupling of radiative cooling, surface fluxes, precipitation, and the circulation (Betts & Ridgway, 1988; Takahashi, 2009). While it is known that RCE is a valid approximation of the global atmosphere, little is known about its applicability on smaller scales. Climate model studies suggest that changes in radiative cooling only correlate well with changes in precipitation for length scales greater than 10,000 km (Muller & O'Gorman, 2011), but those findings are limited by model fidelity and only relate to changes, rather than the mean state.

While the concept of RCE has long been used as a simple framework for investigating the behavior of moist convection (Held et al., 1993; Robe & Emanuel, 1996; Posselt et al., 2008; Singh & O'Gorman, 2013; Tompkins & Craig, 1998), the recognition that, under certain circumstances, convection in RCE can become organized has led to renewed interest in the topic. In particular, simulations of RCE with cloud-resolving models, when run in domains as small as a few hundred kilometers across, are known to spontaneously generate a highly localized and well-organized center of convection surrounded by mostly clear skies, a phenomenon now known as convective aggregation (Bretherton et al., 2005; Grabowski et al., 1996; Held et al., 1993; Tompkins & Craig, 1998). Many cloud-resolving studies have investigated the physical mechanisms and sensitivities of this result to model configuration (Hohenegger & Stevens, 2016; Jeevanjee & Romps, 2013; Muller & Held, 2012; Wing & Emanuel, 2014) including the size of the model domain (Wing & Cronin, 2016) as recently summarized by a number of reviews (Muller & Bony, 2015; Wing et al., 2017). Others have investigated similar behavior of convective aggregation in general circulation models run in RCE in both rotating (Held & Zhao, 2008) and nonrotating frameworks (Bony et al., 2016; Held et al., 2007; Popke et al., 2013; Silvers

et al., 2016). The large variety of results from those studies and the need for a more coordinated effort in understanding them have led to the establishment of the RCE Model Intercomparison Project (Wing et al., 2018), a major community effort to provide further insight into the role and mechanisms of aggregation in organizing convection.

Despite its widespread use in model studies on scales ranging from global to a few hundred kilometers, little is known about RCE from observations, including the scales on which it applies and its relationship to the structure of convection. Gaining this knowledge is critical for ascertaining what can and cannot be inferred from idealized modeling studies. Making use of recent advances in the provision of long-term global data sets, it is the purpose of this study to narrow that gap. Given our interest in the role of convection, we focus on tropical latitudes. Specifically, we apply daily global data sets of radiative fluxes from the Clouds and the Earth's Radiant Energy System (CERES) data set (Kato et al., 2018; Wielicki et al., 1996), precipitation from the Global Precipitation Climatology Project data set (Huffman et al., 2001), sensible heat fluxes from the National Center for Environmental Prediction (NCEP) reanalysis data set (Kalnay et al., 1996), and cloud state information from the International Satellite Cloud Climatology Project (ISCCP) data set (Rossow & Schiffer, 1991) to answer the following questions:

1. At what spatial and temporal scales is the tropical atmosphere near RCE?
2. How do different regions of the tropical atmosphere contribute to RCE?
3. When the tropical atmosphere is in RCE, what role might organized convection play in its maintenance?

To answer these questions, the paper is structured as follows. Section 2 describes the data sources and methodology. Section 3 focuses on investigating the spatial and temporal scales at which the tropical atmosphere is in RCE and on the contribution of different regions to the tropics-wide heat budget. It then investigates the relationship of RCE and organized convection. This is followed by conclusions drawn in section 4.

2. Data and Methods

To evaluate the extent to which the atmosphere may be considered to be in RCE at different spatial and temporal scales, we evaluate the vertically integrated heat budget of the atmosphere. A common expression of this budget at a single location is the equation for vertically averaged dry static energy, $< s >$, where the brackets indicate the vertical average.

$$\frac{\partial < \rho s >}{\partial t} = - < \nabla \rho s \vec{v} > + < Q_R > + LP + H. \quad (1)$$

The dry static energy is defined as $s = c_p T + gz$, where c_P is the specific heat at constant pressure, T is the temperature, g is the gravitational acceleration, and z is height. ρ is the air density, and $\vec{v}$ is the three-dimensional wind vector. $< Q_R >$ is the vertically integrated radiative cooling, LP represents the vertically integrated latent heating, where L is the latent heat of evaporation and P the precipitation, and H is the surface sensible heat flux. The left-hand side of this equation describes local changes in the vertically integrated heat content of the atmosphere, which over long time scales can be assumed to be close to zero (Neelin & Held, 1987). The right-hand side of the equation states that in the absence of changes in local heat content, there exists a balance between four terms, the vertical integral of the divergence of the flux of dry static energy, $< \nabla \rho s \vec{v} >$, the vertically integrated radiative cooling, $< Q_R >$, the vertically integrated latent heating, LP, and the surface sensible heat flux, H.

RCE is a special case of this equilibrium. It assumes a balance of the last three "thermodynamic" terms only, thereby implying the absence of any divergence of the flux of dry static energy. In strict terms, RCE requires that the heat content and flux-divergence terms are identically zero. Here we focus on atmospheric states that are near-RCE, which we define as states in which the sum of the thermodynamic terms are smaller than ± 50 W/m^2 in magnitude. This definition allows for observational uncertainties and the recognition that an exact balance cannot be expected except in the global average and over very long time scales. We chose the value of 50 W/m^2 based on daily grid-point values of latent heating, which often exceed 500 W/m^2 ($\approx$17 mm/day of precipitation). None of our main conclusions are significantly affected by the exact choice, as long as it remains within the same order of magnitude (tens of watts per square meter).

We estimate the radiative cooling of the atmosphere by using daily radiative flux estimates at the top of the atmosphere and the surface provided by the CERES data set (Wielicki et al., 1996). Specifically, we use

daily estimates of top of the atmosphere and surface radiative fluxes at $1° \times 1°$ resolution from the SYN1deg product edition 4a (Kato et al., 2018). This product combines the CERES flux measurements made by the polar-orbiting Terra and Aqua satellites with information from geostationary satellites. We calculate the vertically integrated radiative cooling as $Q_R = R_{\mathrm{TOA,net}} - R_{\mathrm{SFC,net}}$, where $R_{\mathrm{TOA,net}}$ and $R_{\mathrm{SFC,net}}$ are the net radiation fluxes at the top of the atmosphere and surface, respectively. We use 9 years of data covering the years 2001 to 2009.

We match the daily radiative cooling with observations of precipitation at the same temporal (daily) and spatial ($1° \times 1°$) resolution from the Global Climatology Precipitation Project data set (version 1.2) for the same time period (Huffman et al., 2001). We convert the precipitation flux to atmospheric heating by multiplying the rain rates with the latent heat of vaporization using the approximate relationship of $P_E \approx L \times P/86,400$, where P is the precipitation flux in millimeters per day and L is the latent heat of evaporation, so that P_E denotes the precipitation converted to units of energy flux (watts per square meter).

Sensible heat flux and vertical motion estimates are taken from the NCEP Reanalysis project (Kalnay et al., 1996). While constituting estimates from a numerical model constrained by observations, rather than observations, this data set provides a sufficient first-order representation of both the relatively small contributions of the sensible heat fluxes to RCE and the qualitative distribution of vertical motion across the tropics.

One of the goals of this study is to determine the distribution of cloud states present when the atmosphere is near RCE. To do so, we take advantage of the data set of cloud regimes derived from the ISCCP D1 data set (Rossow & Schiffer, 1991). This identification of cloud regimes, also known as weather states, relies on a cluster analysis of daily ISCCP cloud-top pressure versus cloud optical thickness histograms in 280 km by 280 km regions in the tropics (Jakob & Tselioudis, 2003; Rossow et al., 2005). Several studies (Jakob & Schumacher, 2008; Lee et al., 2013; Tan et al., 2013, 2015) have shown that this data set allows for a successful identification of organized, disorganized, and suppressed convective states.

All but the ISCCP cloud regime data set are available to us from 2001 to 2009, which will be our main period of investigation. When assessing cloud regime influences on RCE, we will reduce the period by 1 year until the end of 2008. It will become evident from our results that the sample sizes implied are more than sufficient to support our conclusions.

3. Results

3.1. Tropical RCE: An Overview

We first calculate the 9-year average spatial distribution of the thermodynamic cooling and heating terms of the heat budget (equation (1) and Figure 1). Averaging these contributions over the entire tropics (30°N to 30°S) yields the values of $Q_R = -104.5\ \mathrm{W/m^2}$, $LP = 85.2\ \mathrm{W/m^2}$, and $H = 22.6\ \mathrm{W/m^2}$. This implies an imbalance of the three terms of $3.3\ \mathrm{W/m^2}$, which represents both possible transports in and out of the region as well as measurement uncertainty. Given the small residual compared to the size of the cooling and heating terms themselves, we conclude that in the 9-year average, the tropics as a whole, defined as the region between 30°N and 30°S, are close to RCE. We note that this imbalance is a factor of 3–4 smaller than estimates of atmospheric heat transport from the tropics (Trenberth & Caron, 2001; Wunsch, 2005), highlighting the measurement uncertainties that motivate us to study states near, rather than in exact, RCE.

While the 9-year average over the extended tropics is near RCE, *locally*, the atmosphere is far from equilibrium almost everywhere in this region (Figure 2a). In the precipitating tropics, characterized most clearly by the Intertropical Convergence Zone (ITCZ), the heating by precipitation far outweighs the radiative cooling. Indeed, the radiative cooling tends to be at a minimum in regions where precipitation is maximized. This is the result of the tight connection between precipitation and upper-tropospheric cloudiness, both of which are produced by the convective cloud systems that are typically found in the ITCZ. The presence of upper-tropospheric clouds inhibits the atmosphere from cooling efficiently, as they raise the effective emission level of longwave radiation to space while having relatively little effect on the downwelling longwave radiation at the surface, which remains dominated by emissions from the large water vapor amounts and clouds present at low levels. In contrast, the regions away from the ITCZ are characterized by little to no precipitation accompanied by relatively high values of radiative cooling producing an imbalance in the thermodynamic terms of the heat budget of opposite sign to that found in the ITCZ.

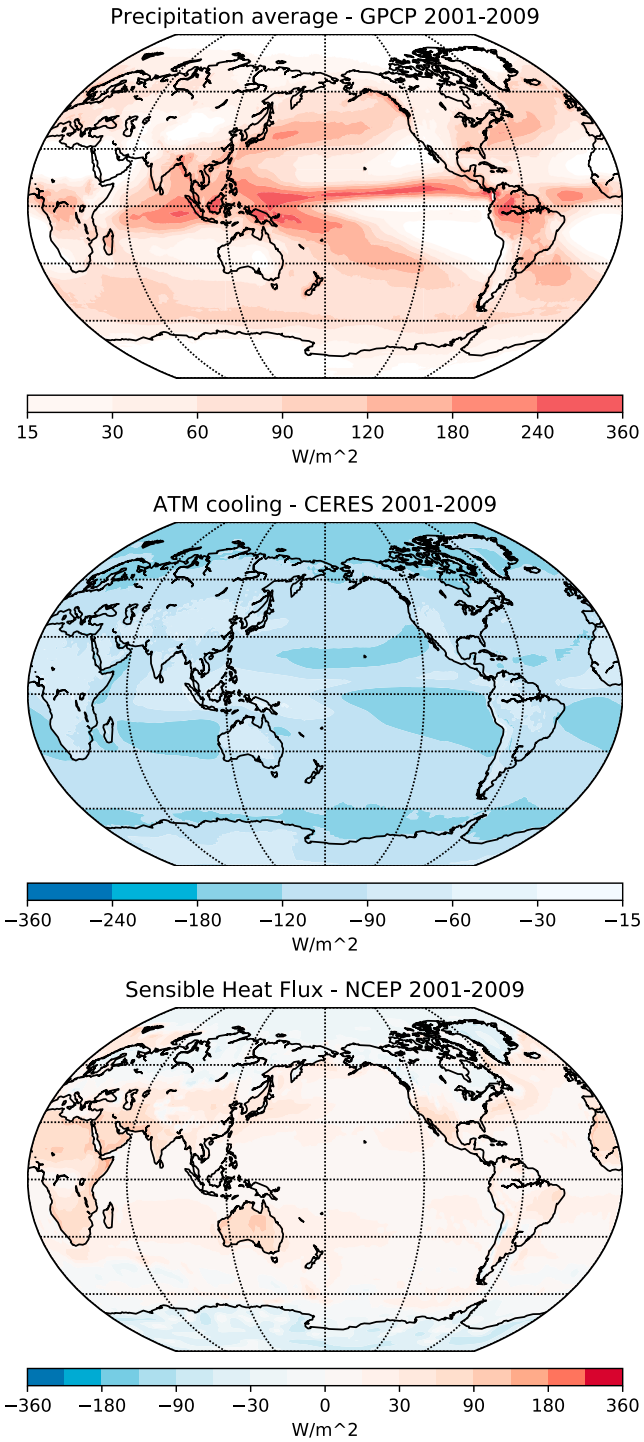

Figure 1. Nine-year average precipitation expressed in energy units (P_E, top), radiative cooling (middle), and sensible heat flux (bottom). GPCP = Global Precipitation Climatology Project; CERES = Clouds and the Earth's Radiant Energy System; NCEP = National Center for Environmental Prediction; ATM = Atmosphere.

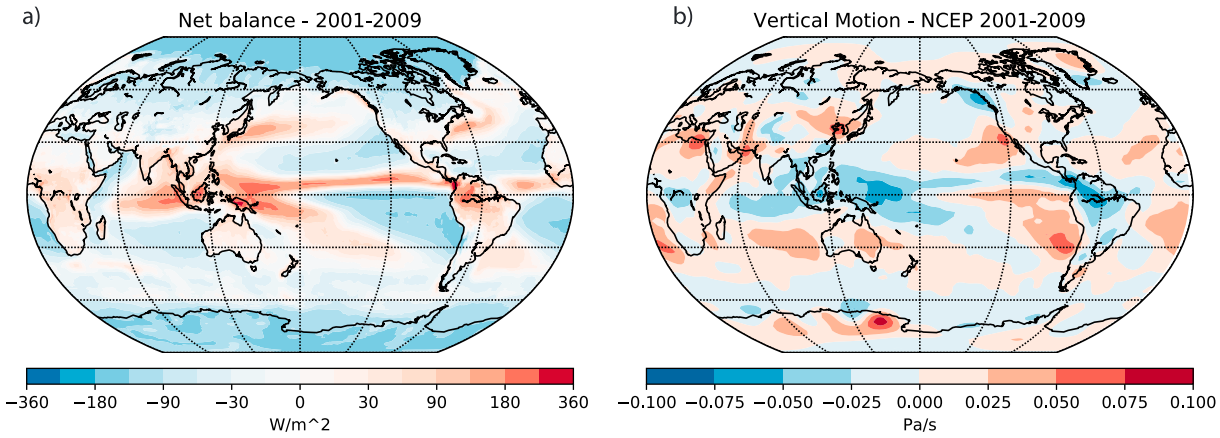

Figure 2. Nine-year average imbalance of radiative cooling, precipitation, and sensible heat flux (a) and mean 500-hPa pressure vertical motion (b). NCEP = National Center for Environmental Prediction.

The agent that connects regions of energy surplus with those of energy deficit is the circulation, as evidenced by Figure 2b. Regions of energy surplus are associated with upward vertical motion (adiabatic cooling), while those with energy deficits are associated with downward motion (adiabatic heating). This highlights the crucial role of circulations in allowing the atmosphere to remain locally in a state far from RCE over long time scales. We note that the vertical motion in Figure 2 is an estimate from the NCEP reanalysis, and as a result, we do not expect a perfect match to the observations. Instead, we use it to qualitatively show the important link of the local "thermodynamic" disequilibrium to circulations. In our further discussions, we implicitly acknowledge this link whenever we find locations and time periods that are away from RCE, which we continue to define as a balance between radiation, precipitation, and sensible heat.

Another way to illustrate the local departures from RCE is a two-dimensional histogram of colocated occurrences of precipitation and radiative cooling (Figure 3), which is constructed using each point in the tropics from the 9-year averages shown in Figure 1. The histogram quantifies our visual impressions discussed above. The vast majority of tropical points is characterized by strong radiative cooling with little to no rainfall (region 1). The next most populated class is one of intermediate precipitation and significant cooling (region 3). There is an interesting secondary maximum of points of low to no rainfall and low-cooling rate (region 2). States of high rainfall and high cooling are nonexisting. In fact, there is a discernible anticorrelation between the two for high rainfall amounts (region 5). This clearly indicates that RCE is a strongly nonlocal feature of the tropical atmosphere. To further illustrate this, we show the geographical location of each of the regions in the histogram on a map (Figure 4).

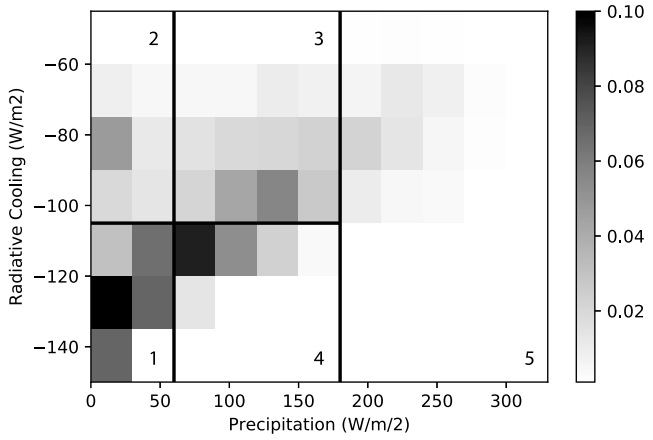

Figure 3. Two-dimensional histogram of the relative frequency of occurrence of combinations of 9-year average precipitation in energy units (P_E) and radiative cooling. Each entry is a grid point. The total number of grid points is 22,320.

We defined two regions of low precipitation in the histogram, one with strong cooling (region 1) and one with weak cooling (region 2). As expected from Figure 1, the strong cooling regions (red) are located over the subtropical oceans, in particular their eastern halves. These regions are dominated by strong subsidence, leading to a dry middle and upper troposphere and a shallow layer of very high humidity accompanied by low-level clouds (Klein & Hartmann, 1993). This leads to relatively high outgoing longwave radiation as well as high downward longwave radiation at the surface and hence low net longwave surface radiation (not shown), giving rise to large cooling. The regions of low rainfall and low atmospheric cooling (orange) are represented by the main desert regions of earth. Here the lack of low-level water vapor significantly reduces the downward longwave radiation, giving rise to the higher radiative energy gain by the atmosphere from the surface and hence less radiative cooling. Given the substantial geographic extent of the desert regions, it is evident that they play a key role in determining the overall heat budget of the tropics, and therefore, desert regions play an important role in setting the tropical-mean precipitation rate.

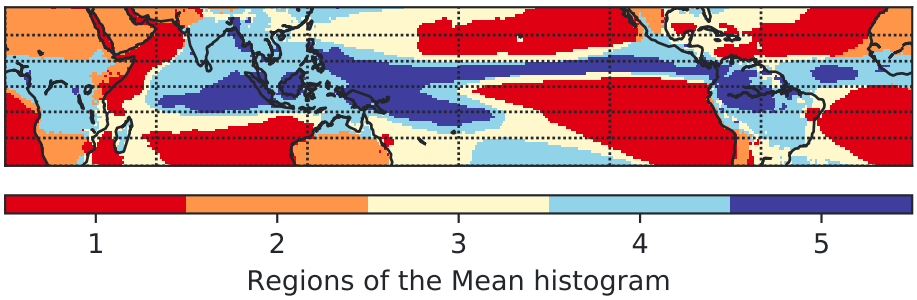

Figure 4. Map of the geographic location of the five regions in the climatological cooling versus precipitation histogram.

The high-precipitation regions (dark blue) map out the center of the ITCZ and are straddled by the medium precipitation low-cooling regions (light blue). Regions of medium precipitation and high cooling (yellow) are found at the outer edges of the ITCZ as well as reaching into the extratropics in the western halves of the ocean basins.

The preceding results reveal that RCE is achieved on a tropics-wide basis through the combination of regions of active convection and suppressed regions, much in the spirit of the furnace-radiator fin model of Pierrehumbert (1995). The following sections will investigate the spatial and temporal scales of the transition to RCE as well as the cloud systems involved in achieving it.

3.2. The Scales of Observed RCE

We begin our investigation by comparing the atmospheric radiative cooling to its heating by precipitation and the sensible heat flux for the entire tropical and subtropical belt (30°N to 30°S) on daily time scales (Figure 5). The heating and cooling are in near-equilibrium every day of the 9-year period under investigation. In other words, the "tropics" as defined above are close to RCE every day. Deviations are on the order of ± 20 W/m^2 for precipitation and ± 10 W/m^2 for radiation. This is obviously larger than the 3 W/m^2 imbalance in the 9-year average. While we would expect balance between heating and cooling on climatological time scales, the fact that most days are quite close to it is remarkable.

We contrast the behavior of the tropics as a whole to an area of $20° \times 20°$centered on the equator in latitude and 185°E in longitude (Figure 6). We see that in this area, which is still ≈2,000 km on a side, the atmosphere is only infrequently near RCE on a daily time scale. In fact, we observe a behavior that is opposite to RCE, in that larger amounts of rainfall are accompanied by a reduction in radiative cooling. This is not surprising and simply highlights the importance of atmospheric dynamic processes on the scales of a few thousand kilometers in setting both the amount of precipitation and the associated radiative cooling. Similar positive

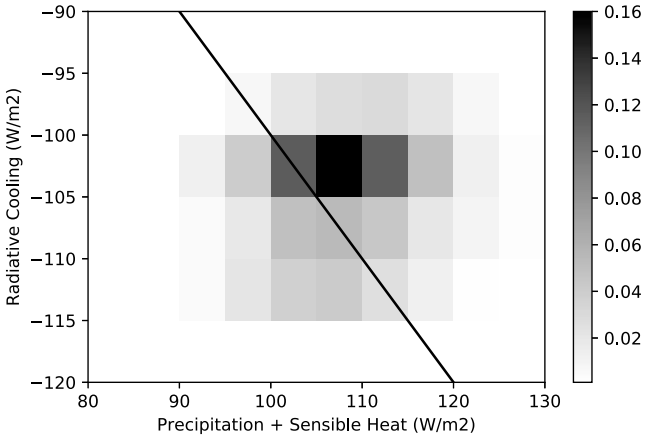

Figure 5. Two-dimensional histogram of the relative frequency of occurrence of combinations of daily tropical-mean precipitation plus sensible heat flux (x axis) and net radiative cooling (y axis). The total sample size is 3,287 days.

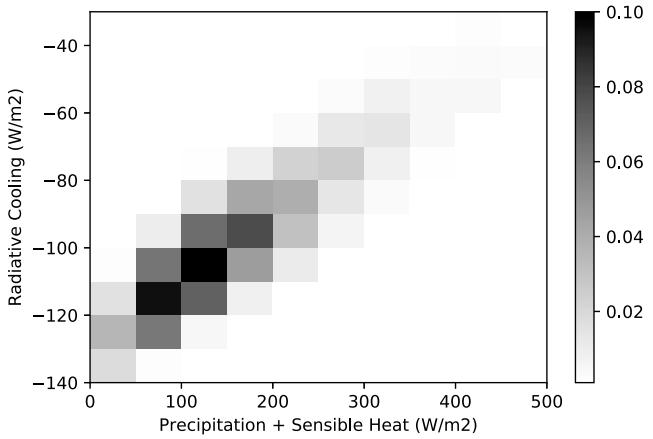

Figure 6. Two-dimensional histogram of the relative frequency of occurrence of combinations of daily mean precipitation plus sensible heat flux (x axis) and net radiative cooling (y axis) for an area of 20° by 20° centered on the equator and 185° E. The total sample size is 3,287 days.

relationships between column net heating and low-level convergence have been found in studies examining the moist static energy budget of the tropical atmosphere (Neelin & Held, 1987).

To investigate the scale dependence of the occurrence of RCE, we define a "distance to RCE." We use the simplest distance estimate possible, namely, the difference between the energy flux from precipitation, the atmospheric radiative cooling, and the surface sensible heat flux, that is, $D_{\mathrm{RCE}} = LP + < Q_R > + H$. Note the sign convention of heat added to the atmosphere as positive resulting in the plus sign in front of the (negative) radiative cooling term. While simple, we will show below that this measure provides insight into the atmosphere's closeness to RCE for different spatial and temporal scales. As we cannot distinguish between deviations due to transports into or out of the tropical domain and data uncertainty, we will allow for a significant difference of ±50 W/m^2 between heating and cooling to be referred to a state near RCE.

We begin our investigation using domains around the grid point in the Pacific already used in Figure 6. We will show the behavior in other regions below. The probability density function of the distance measure at the individual grid point (representing a 1° by 1° area) is highly skewed (Figure 7). At the particular point shown (0°N, 185°E), most days show a negative distance, indicating that the radiative cooling outweighs the heating from precipitation. This highlights the intermittent nature of precipitation over the tropical oceans. The strong skewness of the distribution highlights the very important fact that when rainfall occurs, its heating outweighs the radiative cooling by an order of magnitude, in this case reaching values of up to 2,000 W/m^2 (≈70 mm/day). This contrasts the radiative cooling, which is strongly bounded by vertical structure of temperature, water vapor, and clouds, and rarely exceeds absolute values of 150 W/m^2. This high asymmetry of the rainfall-to-cooling relationship is crucial to the physics of RCE, and we shall return to it later.

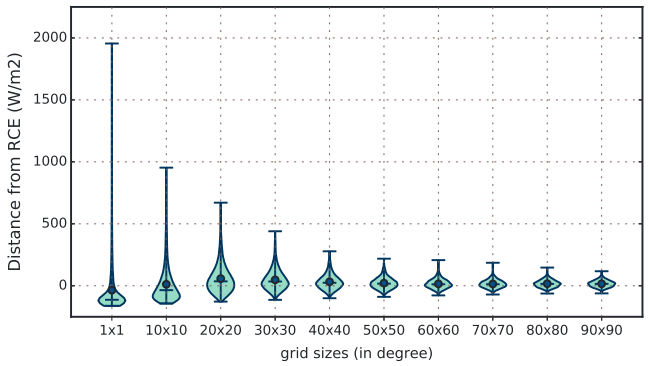

Figure 7. Violin diagram of the distance to RCE for daily input variables as a function of averaging area (in degrees). Results are shown for the grid point centered on the equator and 185° E. Dots represent the mean value, while the horizontal dash indicates the median. RCE =radiative convective equilibrium.

As the scale of spatial averaging increases, the skewness of the distribution of the distance from RCE reduces, and the median values approach zero. Note that the change from negative to positive median at 20° by 20° averaging scale is the result of the location of the point in the relatively cold waters of the equatorial Pacific, straddled by the rain bands of the northern hemisphere ITCZ and southern hemisphere South Pacific Convergence Zone (SPCZ) on both sides. By the time the averaging scales reach ≈50° (or 5,000 km), most values (days) are close to RCE, and both the median and mean of the distance distribution approach zero.

An alternative way to show the increasing closeness to RCE with spatial scale of averaging is to calculate the fraction of days that are near RCE (Figure 8). As discussed above, we apply a loose definition of closeness to RCE by demanding that the RCE distance, D_{RCE}, lies within ±50 W/m^2.

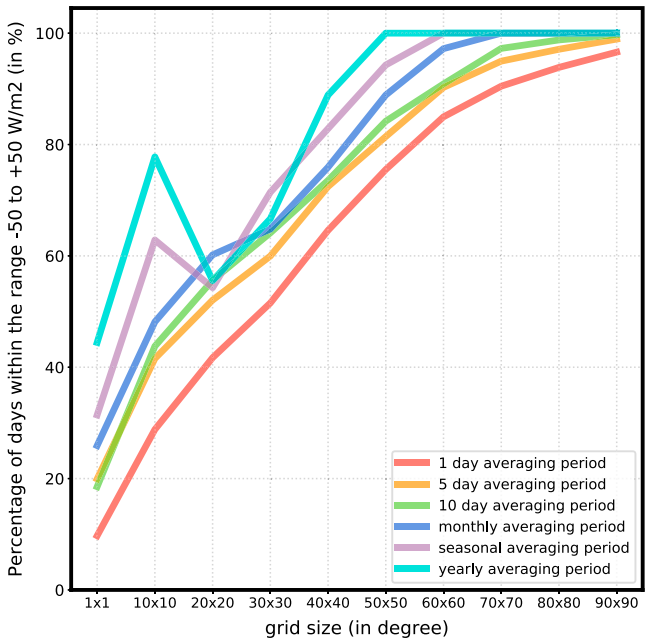

Figure 8. Percentage of time periods that are near radiative convective equilibrium ($|D| < 50 W/m^2$) as a function of averaging scale. The data shown are centered on a point at 0° N and 185° E.

While this range is subjectively chosen with small space and time scales in mind, as we will show below, it provides a good qualitative characterization of RCE behavior. Note that with this definition, the tropics as a whole would be deemed to be near RCE every day in our record (see Figure 5).

Figure 8 shows that for daily averages, the fraction of days in RCE increases from a very small value of ≈10% at the 1° (≈100 km) scale to nearly 90% at 90° (≈9,000 km). Points of note in the evolution of closeness to RCE are the scale of 30°, where the region is in RCE about 50% of the time, and that of 60°, where RCE occurs more than 4 out of 5 times. In other words, when considering daily time scales, frequent RCE requires averaging over length scales of at least 5,000 km.

Time averaging has a much smaller impact on the frequency of RCE than does spatial averaging (Figure 8). Averaging over 5 to 10 days increases the occurrence of RCE by about 10% for each of the spatial resolution. Monthly averaging adds another 10% approximately. For even longer time averages, the evolution of the frequency of RCE with spatial averaging becomes nonmonotonic, with local minima of frequency between length scales of 20°. This is once again the result of the particular location chosen. At the averaging scales of 20°, the region includes the two rain bands of the ITCZ and SPCZ to the north and south of the equator, making it more difficult to be in RCE as much of the domain is covered in heavy precipitation and thick cloud, making radiative cooling inefficient. These rain bands occur as an identifiable structure only in long-term averages and hence do not affect the results for shorter time averages.

As the location of the averaging region clearly influences the results, we repeat the calculations for several locations along the equator. While all regions show the same qualitative behavior of an increase of the fraction of days in RCE with spatial averaging, there are some significant quantitative differences in the rate of increasing RCE frequency with spatial averaging scale (Figure 9). Most prominently, the regions of the Maritime Continent and Eastern Indian Ocean display the slowest rates of RCE frequency increase, while the Atlantic region shows a rather rapid increase. The Pacific Ocean location used so far lies between those two extremes. The two major land regions of Central Africa and the Amazon show a rather slow increase in RCE frequency for length scales less than 30°, with a rapid increase once averaging scales exceed this threshold, most likely due to the increasing inclusion of ocean and desert regions in the averaging. Despite the significant variability across regions, the overall behavior of increasing RCE frequency with averaging is evident in all of them. This indicates that achieving the mixture of heavy precipitation with little cooling and no precipitation with strong cooling that was evident in the overall behavior of the tropics requires large spatial scales to be achieved frequently in time. This raises the question how this mixture of small areas of strong heating and large areas of moderate cooling is achieved and what role convective clouds may play in it.

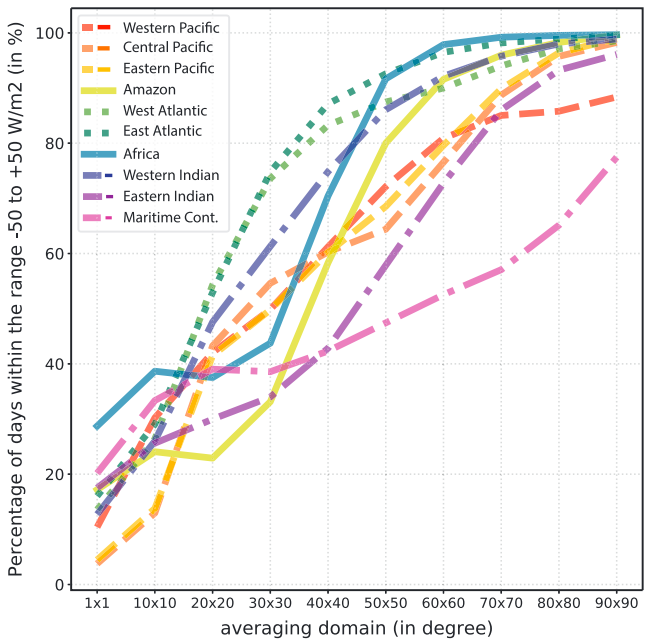

Figure 9. Percentage of time periods that are near radiative convective equilibrium ($|D| < 50 W/m^2$) as a function of averaging scale for different regions of the globe. All regions are centered on the Equator, with the following longitudes in order of the legend: 185° E, 235° E, 265° E, 295° E, 330° E, 0° E, 25° E, 55° E, 85° E, and 125° E.

3.3. RCE and Organized Convection

To better understand how RCE is achieved, we investigate the prevalent cloud types present when it exists. To do so, we apply a cloud regime classification based on ISCCP data (see section 2). This classification analyzes the statistical characteristics of cloud mixtures on a length scale of ≈280 km to identify eight different cloud regimes in the tropical region (see Rossow et al., 2005, and Tan et al., 2013, for more details). Based on the studies above, we distinguish four convectively active types of convection, namely, deep organized convection (CD); deep, but less organized,

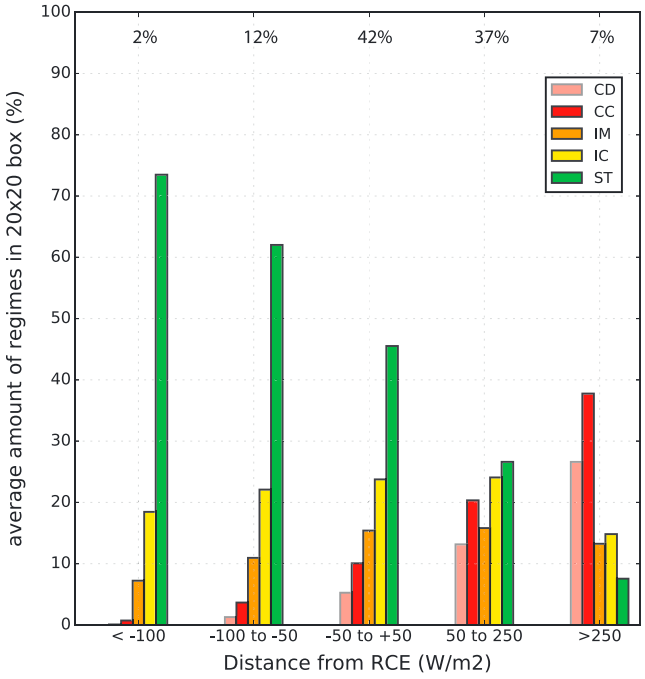

Figure 10. Frequency of occurrence of International Satellite Cloud Climatology Project cloud regimes for five classes of distance to D_{RCE} for the 20° length scale centered on 0° N and 185° E. Numbers near the top indicate the frequency of occurrence of each class. RCE = radiative convective equilibrium; CD = deep organized convection; CC = deep, but less organized, convection; IM = intermediate-depth convection; IC = thin cirrus near decaying convection; ST = four types into a single suppressed cloud regime.

convection (CC); intermediate-depth convection (IM); and thin cirrus near decaying convection (IC). The suppressed cloud types in the original classification comprise a trade cumulus type and three different states of stratocumulus and its transition to cumulus (Rossow et al., 2005). Here we combine these four types into a single suppressed cloud regime (ST).

Starting with results at the 20° (≈2,000 km) length scale for the region we used above (centered on 0° N and 185° E), we calculate the spatial frequency of occurrence of each of the above cloud states for different classes of the distance to RCE on a given day (Figure 10). Large negative distances from RCE (radiative cooling dominates) are characterized by an almost exclusive occurrence of the suppressed cloud states with a relative frequency of more than 70%. Thin cirrus does occur at times as well (≈20%), but the active convective states are virtually absent with the exception of the very occasional (≈8%) occurrence of intermediate-depth convection. Not surprisingly, situations in which the distance to RCE is large and positive (latent heating dominates) are dominated by active convection. Here the organized (CD) and nonorganized (CC and IM) convective states are the most frequent, occurring roughly 65% of the time, and the suppressed state is rare with an occurrence of less than 10%.

For the situations deemed to be near RCE, which at this length scale comprises ≈40% of all days, there is a notable presence of a distinct mixture of the cloud regimes. The most frequent type remains the suppressed cloud state (ST) with an occurrence of about 45%. The second most frequent regime is the thin, most likely detached, cirrus regime (IC), with near 25% of occurrence. The remaining 30% of occurrence are made up of active convection. Here organized convection (CD) occurs about 5% of the time, which is close to its global average (Tan et al., 2013). The CD regime produces significantly more rainfall than any other convective regime (Jakob & Schumacher, 2008). Globally, while occurring only 5% of the time, it produces half the tropical precipitation (Tan et al., 2013). As a result, RCE states cannot be associated with a significant presence of this regime, as that would lead to atmospheric heating that cannot be compensated sufficiently by radiative cooling in suppressed states within the same region.

The lesson learned from the above discussion is that both suppressed and convectively active cloud states, in particular organized deep convection, locally inhibit the atmosphere to be near RCE. In suppressed states,

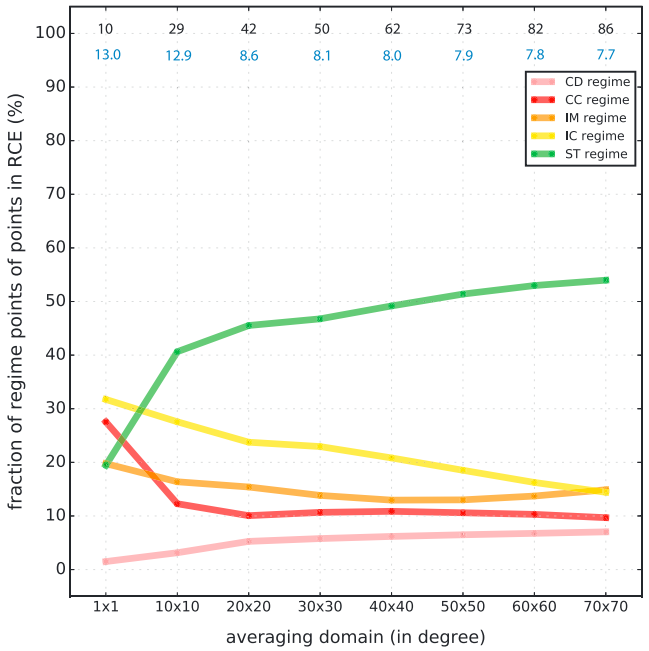

Figure 11. Frequency of occurrence of International Satellite Cloud Climatology Project cloud regimes for the near-RCE class as a function of averaging scale for areas centered on 0° N and 185°E. Black numbers near the top indicate the fraction of days in this class, while blue numbers are the ratio of the frequency of occurrence of ST and that of the CD regime. RCE = radiative convective equilibrium; CD = deep organized convection; CC = deep, but less organized, convection; IM = intermediate-depth convection; IC = thin cirrus near decaying convection; ST = four types into a single suppressed cloud regime.

the radiative cooling dominates over net latent heating, while in active states, the latent heating from precipitation far outweighs the cooling. As discussed earlier, the dominance is not symmetric around zero, as the radiative cooling is limited to values of ≈150 W/m^2, while the latent heating can be an order of magnitude larger. Also, as seen in Figure 1, on average, the precipitating regions themselves, through their association with high clouds, become inefficient in cooling radiatively. It is therefore not surprising that days that are found to be near RCE are characterized by a mix of active and suppressed states of cloudiness, with the suppressed states the most frequent and the strongly precipitating organized convective states the rarest. However, we have so far only shown this to be true for length scales of ≈2,000 km.

Extending our investigation of cloud regime mixtures near RCE to different averaging scales reveals several interesting results (Figure 11). At scales larger than 2,000 km, where RCE occurs more than 50% of the time, the days in RCE are characterized by a cloud state mixture that is qualitatively similar to the one described above. In all cases, the suppressed cloud states dominate the mixture, increasing to just above 50% for larger scales. This increase occurs mostly at the expense of the thin cirrus regime, probably indicative of the fact that the averaging area on small scales includes mainly the deep tropics, while large areas increasingly include subtropical regions. A striking feature of the cloud mixture evolution with scale is that, while the number of occurrences of RCE increases with scale (black numbers in Figure 11), the ratio of the suppressed state and that of organized convection remains nearly constant (blue numbers in Figure 11). This indicates that to be in RCE, there is an "ideal" mixture of relatively small coverage with heavily precipitating organized convection and large regions covered by suppressed conditions.

In the light of the recent frequent use of the RCE assumption on scales of a few hundred kilometers, it is worth highlighting another result from Figure 11. First, as already discussed above, areas of that scale are very rarely in RCE (≈10% of the days in our sample). Second, when they are, the cloud mixture that is encountered in such areas is very different from those at larger scales. Notably, organized convection is virtually absent, and the suppressed states occur rarely as well. This is consistent with our conclusion that both these states locally inhibit RCE. Instead, small-scale RCE is characterized by the unorganized convective states as well as the thin cirrus state. This is understandable as achieving RCE requires precipitation and radiative cooling to balance and therefore limits the precipitation to relatively small values of 2–3 mm/day. A second requirement is that the atmosphere remains relatively efficient at cooling, which prohibits the existence of thick high clouds. Putting the two requirements together explains why it is unorganized convection, with likely small rain rates and no significant anvil generation, that is the dominant cloud type in RCE at small scales.

4. Conclusions

This study investigates the behavior of the tropical atmosphere in the context of the well-known paradigm of RCE. We apply a number of observational data sets with the aim of quantifying the temporal and spatial scales at which RCE manifests in Earth's tropical atmosphere. We also investigate the role of different cloud states in contributing to RCE across scales. We account for the significant observational uncertainty, especially in surface radiation, by developing a "distance from RCE" measure and by considering states that are near RCE rather than in strict RCE.

We find that in a multiyear average, the tropical atmosphere, defined here as 30°N to 30°S, is within a few watts per square meter of balance between radiative cooling, precipitation, and sensible heat input from the surface. We show that the same balance does not hold locally even for long-term temporal averages. We quantify from observations the relative contributions to tropics-wide RCE from the regions of strong cooling and little rainfall in the subtropics and the convectively active regions in the deep tropics, in which latent

heating far outstrips radiative cooling. We demonstrate that the world's deserts play an important role in the equilibrium as they constitute regions of no rainfall with anomalously low radiative cooling. An Earth without deserts will therefore have higher global-mean rainfall rates, a finding confirmed by the numerous experiments conducted with global models in so-called aqua-planet simulations (Medeiros et al., 2008; Neale & Hoskins, 2000; Williamson & Olson, 2003).

We show that, perhaps surprisingly, the tropics are near RCE on a daily time scale, with imbalances between the contributing terms of a few tens of watts per square meter at the most. However, the likelihood of encountering RCE anywhere in the tropics strongly decreases with decreasing spatial scale. While temporal averaging increases the proportion of points near to RCE, the effect is far less pronounced than for spatial averages. For most regions of the tropics, encountering RCE more than 75% of the time requires averaging scales of several thousand kilometers, while RCE in domains smaller than 1,000 km occurs usually less than 20% of the time. At these smaller scales, the relationship between radiative cooling and precipitation is the reverse of that expected in strict RCE; high-precipitation rates tend to coincide, both spatially and temporally, with relatively low radiative cooling rates. This behavior may be understood by considering the effect of column heating and cooling on the moist static energy budget (Neelin & Held, 1987).

By applying cloud regime information, we show that on large scales (>5,000 km), RCE is the result of a mixture of cloud states with the majority of the area covered in low clouds accompanied by suppressed conditions and a small area covered with active convection. Within the region of active convection, organized convection is a rare state occurring in around 5% of the area, a similar rate to that found in the global average. This finding is consistent with cloud-resolving model studies of convective aggregation in which the convecting region shrinks to a small fraction of the domain as aggregation proceeds (Bretherton et al., 2005; Wing et al., 2017). However, apart from a few notable exceptions (Wing & Cronin, 2016), such studies are performed in domains of only a few hundred kilometers across. In the observations, RCE is rare at such scales (O(100 km)), and when it exists, it is characterized by mostly disorganized convective cloud states (Figure 11).

It is difficult to assess the importance of this discrepancy given the strong idealizations used in RCE model experiments. It is well known that in addition to the radiative and surface flux-driven feedback processes identified in RCE simulations (Muller & Held, 2012; Wing & Emanuel, 2014), the organization of convection in the tropics is affected by a number of other drivers. While much of the attention in RCE simulations is on the role of sea-surface temperature or its gradients in affecting the organization of convection, our study confirms a more complex picture that intimately couples RCE to the global circulation, which both affects and is affected by surface temperature. It is well known that influences on this circulation include horizontal gradients in insolation, sea-surface temperature gradients, the planet's rotation rate, land-sea contrasts, and synoptic disturbances associated with tropical weather. Many of these act on scales larger than a few hundred kilometers, so it is perhaps not surprising that the observed scales of RCE are so large. While there have been studies to investigate the role of individual drivers of convective organization (e.g., Albern et al., 2018; Philander et al., 1996; Reed & Chavas, 2015; Tompkins, 2001; Wing et al., 2016), a comprehensive study that investigates their relative role in a single modeling framework is still lacking. The proposed RCEMIP (Wing et al., 2018) and other intercomparison projects provide an excellent opportunity to more comprehensively investigate the relative importance of the processes that organize tropical convection.

The application of modern, mostly satellite-based, observations to studying thermodynamic equilibria shows much promise in quantifying the relative roles of radiative cooling in the different regions on Earth in constraining tropical-mean precipitation. An obvious next step is to use the findings of this study to investigate the rainfall to cooling relationship in climate models to shed new light on model errors as well as model responses to changes in forcings of the climate system.

Acknowledgments
This work was supported by the ARC Centre of Excellence for Climate Extremes (CE170100023). We thank Adrian Tompkins and two anonymous reviewers for their insightful comments. All data sets are freely available through the respective institutions cited in the text. The CERES data set is available online (https://ceres.larc.nasa.gov/products-info.php?product=SYN1deg). The GPCP data are available online (https://www.ncdc.noaa.gov/cdr/atmospheric/precipitation-gpcp-daily). The NCEP reanalysis data are availabe online (https://www.esrl.noaa.gov/psd/data/reanalysis/reanalysis.shtml). The ISCCP cloud regime data are available online (https://www.noaacrest.org/rscg/Products/WS/tcluster.html).

References

Albern, N., Voigt, A., Buehler, S. A., & Grützun, V. (2018). Robust and nonrobust impacts of atmospheric cloud-radiative interactions on the tropical circulation and its response to surface warming. *Geophysical Research Letters*, *45*, 8577–8585. https://doi.org/10.1029/2018GL079599

Betts, A. K., & Ridgway, W. (1988). Coupling of the radiative, convective, and surface fluxes over the equatorial Pacific. *Journal of the Atmospheric Sciences*, *45*, 522–536.

Bony, S., Stevens, B., Coppin, D., Becker, T., Reed, K. A., Voigt, A., & Medeiros, B. (2016). Thermodynamic control of anvil cloud amount. *Proceedings of the National Academy of Sciences of the United States of America*, *113*, 8927–8932.

Bretherton, C. S., Blossey, P. N., & Khairoutdinov, M. (2005). An energy-balance analysis of deep convective self-aggregation above uniform SST. *Journal of the Atmospheric Sciences*, *62*, 4273–4292.
Grabowski, W. W., Moncrieff, M. W., & Kiehl, J. T. (1996). Long-term behaviour of precipitating tropical cloud systems: A numerical study. *Quarterly Journal of the Royal Meteorological Society*, *122*, 1019–1042.
Held, I. M., Hemler, R. S., & Ramaswamy, V. (1993). Radiative-convective equilibrium with explicit two-dimensional moist convection. *Journal of the Atmospheric Sciences*, *50*, 3909–3927.
Held, I. M., & Zhao, M. (2008). Horizontally homogeneous rotating radiative–convective equilibria at GCM resolution. *Journal of the Atmospheric Sciences*, *65*, 2003–2013.
Held, I. M., Zhao, M., & Wyman, B. (2007). Dynamic radiative-convective equilibria using GCM column physics. *Journal of the Atmospheric Sciences*, *64*, 228–238.
Hohenegger, C., & Stevens, B. (2016). Coupled radiative convective equilibrium simulations with explicit and parameterized convection. *Journal of Advances in Modeling Earth Systems*, *8*, 1468–1482. https://doi.org/10.1002/2016MS000666
Huffman, G. J., Adler, R. F., Morrissey, M. M., Bolvin, D. T., Curtis, S., Joyce, R., et al. (2001). Global precipitation at one-degree daily resolution from multisatellite observations. *Journal of Hydrometeorology*, *2*, 36–50.
Jakob, C., & Schumacher, C. (2008). Precipitation and latent heating characteristics of the major Tropical Western Pacific cloud regimes. *Journal of Climate*, *21*, 4348–4364.
Jakob, C., & Tselioudis, G. (2003). Objective identification of cloud regimes in the Tropical Western Pacific, *30*, 2082. https://doi.org/10.1029/2003GL018367
Jeevanjee, N., & Romps, D. M. (2013). Convective self-aggregation, cold pools, and domain size. *Geophysical Research Letters*, *40*, 994–998. https://doi.org/10.1002/grl.50204
Kalnay, E., Kanamitsu, M., Kistler, R., Collins, W., Deaven, D., Gandin, L., et al. (1996). The NCEP/NCAR 40-Year Reanalysis Project. *Bulletin of the American Meteorological Society*, *77*, 437–471.
Kato, S., Rose, F. G., Rutan, D. A., Thorsen, T. J., Loeb, N. G., Doelling, D. R., et al. (2018). Surface irradiances of edition 4.0 Clouds and the Earth's Radiant Energy System (CERES) Energy Balanced and Filled (EBAF) data product. *Journal of Climate*, *31*, 4501–4527.
Klein, S. A., & Hartmann, D. L. (1993). The seasonal cycle of low stratiform clouds. *Journal of Climate*, *6*, 1587–1606.
Lee, D., Oreopoulos, L., Huffman, G. J., Rossow, W. B., & Kang, I.-S. (2013). The precipitation characteristics of ISCCP tropical weather states. *Journal of Climate*, *26*, 772–788.
Manabe, S., & Strickler, R. F. (1964). Thermal equilibrium of the atmosphere with a convective adjustment. *Journal of the Atmospheric Sciences*, *21*, 361–385.
Medeiros, B., Stevens, B., Held, I. M., Zhao, M., Williamson, D. L., Olson, J. G., & Bretherton, C. S. (2008). Aquaplanets, climate sensitivity, and low clouds. *Journal of Climate*, *21*, 4974–4991.
Muller, C., & Bony, S. (2015). What favors convective aggregation and why? *Geophysical Research Letters*, *42*, 5626–5634. https://doi.org/10.1002/2015GL064260
Muller, C. J., & Held, I. M. (2012). Detailed investigation of the self-aggregation of convection in cloud-resolving simulations. *Journal of the Atmospheric Sciences*, *69*, 2551–2565.
Muller, C. J., & O'Gorman, P. A. (2011). An energetic perspective on the regional response of precipitation to climate change. *Nature Climate Change*, *1*, 266–271.
Neale, R. B., & Hoskins, B. J. (2000). A standard test for AGCMs including their physical parametrizations. II: Results for the Met Office Model. *Atmospheric Science Letters*, *1*, 108–114.
Neelin, J. D., & Held, I. M. (1987). Modeling tropical convergence based on the moist static energy budget. *Monthly Weather Review*, *115*, 3–12.
Philander, S. G. H., Gu, D., Lambert, G., Li, T., Halpern, D., Lau, N.-C., & Pacanowski, R. C. (1996). Why the ITCZ is mostly north of the Equator. *Journal of Climate*, *9*, 2958–2972.
Pierrehumbert, R. T. (1995). Thermostats, radiator fins, and the local runaway greenhouse. *Journal of the Atmospheric Sciences*, *52*, 1784–1806.
Popke, D., Stevens, B., & Voigt, A (2013). Climate and climate change in a radiative-convective equilibrium version of ECHAM6. *Journal of Advances in Modeling Earth Systems*, *5*, 1–14. https://doi.org/10.1029/2012MS000191
Posselt, D. J., van den Heever, S. C., & Stephens, G. L. (2008). Trimodal cloudiness and tropical stable layers in simulations of radiative convective equilibrium. *Geophysical Research Letters*, *35*, L08802. https://doi.org/10.1029/2007GL033029
Reed, K. A., & Chavas, D. R. (2015). Uniformly rotating global radiative-convective equilibrium in the Community Atmosphere Model, version 5. *Journal of Advances in Modeling Earth Systems*, *7*, 1938–1955. https://doi.org/10.1002/2015MS000519
Robe, F. R., & Emanuel, K. A. (1996). Moist convective scaling: Some inferences from three-dimensional cloud ensemble simulations. *Journal of the Atmospheric Sciences*, *53*, 3265–3275.
Rossow, W. B., & Schiffer, R. A. (1991). ISCCP cloud data products. *Bulletin of the American Meteorological Society*, *72*, 2–20.
Rossow, W. B., Tselioudis, G., Polak, A., & Jakob, C. (2005). Tropical climate described as a distribution of weather states indicated by distinct mesoscale cloud property mixtures. *Geophysical Research Letters*, *32*, L21812. https://doi.org/10.1029/2005GL024584
Silvers, L. G., Stevens, B., Mauritsen, T., & Giorgetta, M. (2016). Radiative convective equilibrium as a framework for studying the interaction between convection and its large-scale environment. *Journal of Advances in Modeling Earth Systems*, *8*, 1330–1344. https://doi.org/10.1002/2016MS000629
Singh, M. S., & O'Gorman, P. A. (2013). Influence of entrainment on the thermal stratification in simulations of radiative-convective equilibrium. *Geophysical Research Letters*, *40*, 4398–4403. https://doi.org/10.1002/grl.50796
Takahashi, K. (2009). Radiative constraints on the hydrological cycle in an idealized radiative–convective equilibrium model. *Journal of the Atmospheric Sciences*, *66*, 77–91.
Tan, J., Jakob, C., & Lane, T. P. (2013). On the identification of the large-scale properties of tropical convection using cloud regimes. *Journal of Climate*, *26*, 6618–6632.
Tan, J., Jakob, C., Rossow, W. B., & Tselioudis, G. (2015). Increases in tropical rainfall driven by changes in frequency of organized deep convection. *Nature*, *519*, 451–454.
Tompkins, A. M. (2001). On the relationship between tropical convection and sea surface temperature. *Journal of Climate*, *14*, 633–637.
Tompkins, A. M., & Craig, G. C. (1998). Radiative-convective equilibrium in a three-dimensional cloud-ensemble model. *Quarterly Journal of the Royal Meteorological Society*, *124*, 2073–2097.
Trenberth, K. E., & Caron, J. M. (2001). Estimates of meridional atmosphere and ocean heat transports. *Journal of Climate*, *14*, 3433–3443.
Wielicki, B. A., Barkstrom, B. R., Harrison, E. F., Lee III, R. B., Louis Smith, G., & Cooper, J. E. (1996). Clouds and the Earth's Radiant Energy System (CERES): An Earth observing system experiment. *Bulletin of the American Meteorological Society*, *77*, 853–868.

Williamson, D. L, & Olson, J. G (2003). Dependence of aqua-planet simulations on time step. *Quarterly Journal of the Royal Meteorological Society*, *129*, 2049–2064.

Wing, A. A., Camargo, S. J., & Sobel, A. H. (2016). Role of radiative-convective feedbacks in spontaneous tropical cyclogenesis in idealized numerical simulations. *Journal of the Atmospheric Sciences*, *73*, 2633–2642.

Wing, A. A., & Cronin, T. W. (2016). Self-aggregation of convection in long channel geometry. *Quarterly Journal of the Royal Meteorological Society*, *142*, 1–15.

Wing, A. A., & Emanuel, K. A. (2014). Physical mechanisms controlling self-aggregation of convection in idealized numerical modeling simulations. *Journal of Advances in Modeling Earth Systems*, *6*, 59–74. https://doi.org/10.1002/2013MS000269

Wing, A. A., Emanuel, K., Holloway, C. E., & Muller, C. (2017). Convective self-aggregation in numerical simulations: A review. *Surveys in Geophysics*, *38*, 1173–1197.

Wing, A. A., Reed, K. A., Satoh, M., Stevens, B., Bony, S., & Ohno, T. (2018). Radiative–convective equilibrium model intercomparison project. *Geoscientific Model Development*, *11*, 793–813.

Wunsch, C. (2005). The total meridional heat flux and its oceanic and atmospheric partition. *Journal of Climate*, *18*, 4374–4380.